Human Molecular Genetics, 2007, Vol. 16, No. 7 ***774–782***
doi:10.1093/hmg/ddm022
Advance Access published on March 5, 2007

Trisomy for the Down syndrome 'critical region' is necessary but not sufficient for brain phenotypes of trisomic mice

Lisa E. Olson[1], Randall J. Roper[2,†], Crystal L. Sengstaken[1], Elizabeth A. Peterson[1], Veronica Aquino[2], Zygmunt Galdzicki[3], Richard Siarey[3], Mikhail Pletnikov[2], Timothy H. Moran[2] and Roger H. Reeves[2,*]

[1]University of Redlands, Redlands, CA 92373, USA, [2]Johns Hopkins University School of Medicine, Baltimore, MD 21205, USA and [3]Uniformed Services University of the Health Sciences, Bethesda, MD 20814, USA

Received January 10, 2007; Revised and Accepted February 7, 2007

Trisomic Ts65Dn mice show direct parallels with many phenotypes of Down syndrome (DS), including effects on the structure of cerebellum and hippocampus. A small segment of Hsa21 known as the 'DS critical region' (DSCR) has been held to contain a gene or genes sufficient to cause impairment in learning and memory tasks involving the hippocampus. To test this hypothesis, we developed Ts1Rhr and Ms1Rhr mouse models that are, respectively, trisomic and monosomic for this region. Here, we show that trisomy for the DSCR alone is not sufficient to produce the structural and functional features of hippocampal impairment that are seen in the Ts65Dn mouse and DS. However, when the critical region is returned to normal dosage in trisomic Ms1Rhr/Ts65Dn mice, performance in the Morris water maze is identical to euploid, demonstrating that this region is necessary for the phenotype. Thus, although the prediction of the critical region hypothesis was disproved, novel gene dosage effects were identified, which help to define how trisomy for this segment of the chromosome contributes to phenotypes of DS.

INTRODUCTION

Inheritance of three copies of human chromosome 21 (Hsa21) results in the clinical condition known as Down syndrome (DS). Although most systems are affected to some degree in DS, impaired cognitive function is among the most important effects. Over-expression of genes on Hsa21 in DS is implied from studies in trisomic mouse models that upregulate nearly all trisomic genes by ~50% across many tissues (1,2). There is currently no explanation for how this relatively small increase in transcript levels results in any specific feature of the syndrome.

'Phenotype maps' have been used to correlate expression of specific genes with specific aspects of DS. These are developed from the assessment of persons with segmental trisomy involving only a portion of Hsa21. The smallest chromosomal region in common among individuals who share a given feature is referred to as a 'Down syndrome critical region' (DSCR). The best-defined DSCR extends ~5 Mb from *D21S17* to *MX1* in band 21q22.3. This segment contains about 33 conserved genes (3) and has been associated with DS features including craniofacial abnormalities, short stature, joint hyperlaxity, hypotonia and mental retardation (4,5). This DSCR has also been proposed to contain a gene or genes responsible for 'mental retardation of the DS type', which is characterized by deficits in speech, language, verbal short-term memory, spatial learning and recall and long-term memory. Pennington *et al.* (6) have documented specific effects of DS involving functions of the hippocampus and to a lesser degree, the prefrontal cortex.

In addition to these functional effects, trisomy 21 produces specific structural differences in the DS brain. Reduced volume of the hippocampus is well established in human magnetic resonance imaging (MRI) studies of non-demented adults with DS (7–9). This reduction apparently arises early in development as it is seen in children as well (10). Adults

*To whom correspondence should be addressed at: Department of Physiology, Johns Hopkins University School of Medicine, 725 N. Wolfe Street, Baltimore, MD 21205, USA. Tel: +1 4109556621; Fax: +1 4432870508; Email rreeves@jhmi.edu
†Current address: Department of Biology, Indiana University-Purdue University at Indianapolis, Indianapolis, IN, USA.

with DS exhibit a characteristically reduced cerebellar volume (9,11) and reduction in granule cell density (12). The relationship between specific structural and functional deficits in DS is unclear.

Several phenotypes analogous to those in DS have been established in mouse genetic models (Fig. 1). The Ts65Dn and Ts1Cje mouse models are trisomic for large segments of mouse chromosome 16 (Mmu16), which are conserved with Hsa21. Ts65Dn mice exhibit small body size (13); alterations in the craniofacial skeleton, mandible and cranial vault that correspond directly to those in DS (14) and impaired function in tests of spatial memory that dependent on hippocampus, such as the Morris swim maze (15–17). Ts1Cje mice, which are trisomic for 78% of the genes triplicated in Ts65Dn, have somewhat milder versions of the same spatial memory and craniofacial abnormalities (18,19).

These models also show some anatomical changes in the brain that parallel those in DS. Ts65Dn mice have a reduced cerebellar volume as well as reduced granule cell and Purkinje cell density (12), whereas Ts1Cje mice exhibit a variable severity of these phenotypes in the cerebellum (20). In Ts65Dn mice, the dentate gyrus contains fewer granule cells throughout development at postnatal day 6, in young adults at 3 months of age, and in older adults after the onset of basal forebrain cholinergic neuron degeneration that is characteristic of DS and mouse models (21,22). A significant increase in pyramidal cells in layer CA3 of the *cornus ammonis* has been reported at 5 months but not at 3 months; however, the total cell numbers (CA1 + CA3) are the same as euploid at both ages, suggesting that the difference may be methodological rather than biological (21,22).

Long-term potentiation (LTP) is a form of synaptic plasticity evoked by a train of electrical stimuli, leading to strengthening of synapses between neurons. Hippocampal LTP is considered to be a physiological model of learning and memory. LTP is reduced in the CA1 and dentate gyrus areas of the hippocampus in the Ts65Dn and Ts1Cje mouse models (23–26) and CA1 LTP is reduced in the Tc1 mouse that carries a nearly intact copy of Hsa21 in about half the cells in the adult brain (27).

Quantitation of functional and structural phenotypes in the Ts65Dn and Ts1Cje mouse models has validated the use of mice to study the genetic basis and pathogenesis of DS. Until recently, however, no mouse model existed that was trisomic for solely the DSCR. The Dp(16Cbr1-ORF9)1Rhr (Ts1Rhr) mouse is trisomic only for the subset of mouse genes triplicated in Ts65Dn and Ts1Cje that correspond to the DSCR, i.e. those between *Cbr3* and *Mx2* (Fig. 1). Ts1Rhr and the corresponding segmental monosomy (Ms1Rhr) were created using Cre/LoxP-based chromosomal engineering to produce an unbalanced reciprocal translocation of Mmu16 (20). Ts1Rhr can be assessed directly to determine whether trisomy for the DSCR is sufficient to produce phenotypes seen in Ts65Dn and DS, whereas Ms1Rhr can be bred to Ts65Dn to 'subtract' the DSCR from the larger Ts65Dn trisomic segment to determine whether these genes are necessary (Fig. 1). Analysis of these models has demonstrated that trisomy for the DSCR alone is insufficient and largely not necessary to cause three features attributed to it: short stature, small mandible (which contributes to the protruding tongue) and anomalies of the craniofacial skeleton (28).

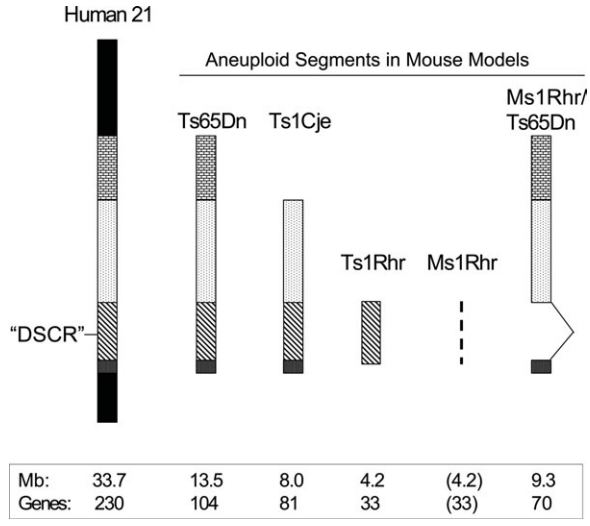

Figure 1. Aneuploid segments in Ts65Dn, Ts1Cje, Ts1Rhr, Ms1Rhr and Ms1Rhr/Ts65Dn mice. The size of aneuploid mouse segments and Hsa21q are based on mouse build 36 (http://www.ensembl.org/mus_musculus/index.html) and build 42 of the human genome (http://www.ensembl.org/homo_sapiens/index.html). The number of 'conserved' and 'minimally conserved' mouse orthologs of Hsa21 genes in each model is based on the data from Gardiner co-workers. (3) (http://chr21db.cudenver.edu/).

Here, we examine structural and functional properties of the brain in Ts1Rhr, Ms1Rhr and Ms1Rhr/Ts65Dn aneuploid mice and genetically matched euploid controls (see Materials and Methods). An unexpected pattern of structural effects is discovered in monosomic Ms1Rhr mice. The DSCR prediction that this region is sufficient to produce mental retardation of the DS type is not substantiated, but dosage imbalance for a gene or genes in this segment makes a necessary contribution to hippocampal-based learning deficits in Ts65Dn.

RESULTS

Whole brain and hippocampal volume in aneuploid mice

We reported previously that the size of the brain overall was not different between Ts65Dn and euploid controls (12). We measured the volume of brain regions using high-resolution three-dimensional MRI in 10 Ts1Rhr animals that are trisomic for the DSCR, 10 Ms1Rhr mice that have segmental monosomy for this region and 11 euploid controls. Overall brain volume was slightly larger than euploid in Ts1Rhr mice (Fig. 2A). In marked contrast, Ms1Rhr mice, which have segmental monosomy for the same genes present in three copies in Ts1Rhr mice, showed a significant reduction in brain volume (85% of euploid). Average body mass in the strains studied here is Ms1Rhr < Ts65Dn < euploid < Ts1Rhr (13,20,28), thus the increase in the brain size in Ts1Rhr mice and decrease in the brain size in Ms1Rhr mice reflect the larger and smaller body size in these two strains, respectively. All cerebellar and hippocampal measurements were normalized to total brain volume to account for differences in overall size between strains.

We calculated the volume of the hippocampus from measurements of area in serial MRI slices. Landmarks were

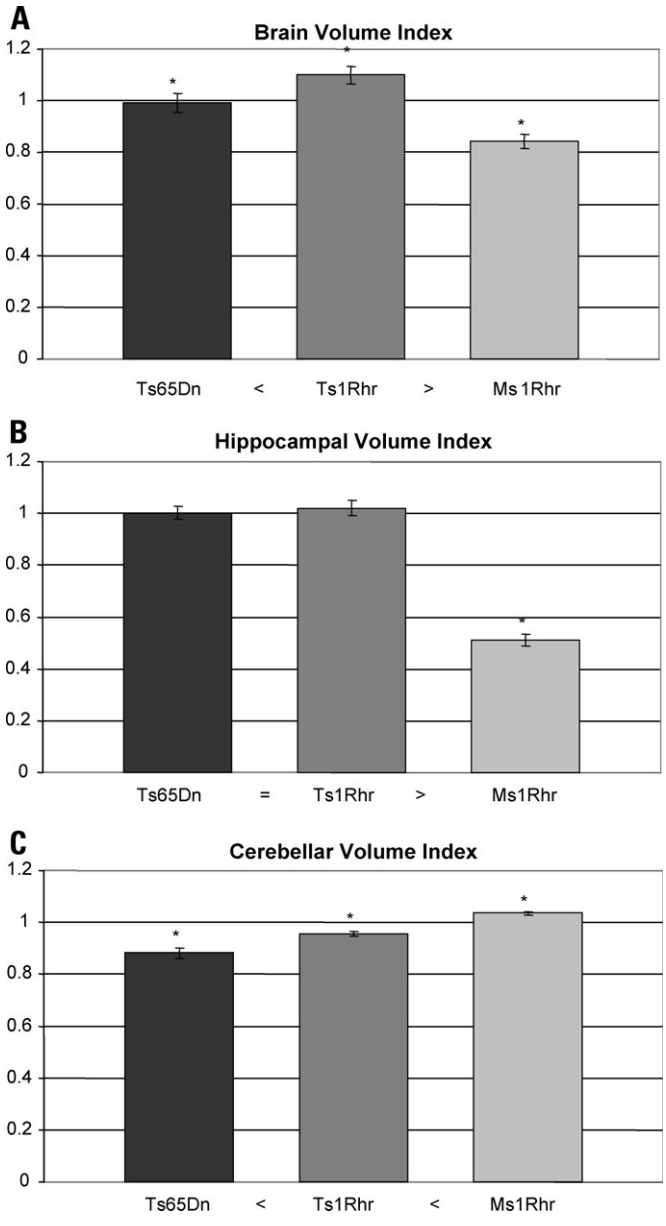

Figure 2. Volumetric and cell density analysis of aneuploid mouse brains (ANOVA and multiple comparisons testing, $\alpha = 0.05$). (**A**) Brain volume index (aneuploid/euploid), Ms1Rhr < Ts65Dn < Ts1Rhr. (**B**) Normalized hippocampus volume index (normalized to whole brain within groups and compared across groups). (**C**) Normalized cerebellum volume index (normalized to whole brain within groups and compared across groups). Asterisks indicate classes that are significantly different, and error bars indicate standard error of mean.

adapted from those established in the rat (29). Volumetric pixels were used to determine hippocampal volume relative to euploid in Ts65Dn, Ts1Rhr and Ms1Rhr models. Effects of each aneuploid genotype were compared with euploid using a *t*-test (Table 1), and between strain, comparisons were evaluated by multiple comparisons testing (Fig. 2). When hippocampal volume was normalized to overall brain volume, neither Ts65Dn nor Ts1Rhr was different from euploid (Table 1 and Fig. 2B). In contrast, Ms1Rhr has a markedly smaller hippocampus (51% of euploid volume, $P < 0.001$) even relative to the small overall brain volume.

Ts1Rhr cerebellum shows a mild reduction in volume but normal granule and Purkinje cell density

The volume of the Ts65Dn brain is the same as that of euploid, but its cerebellar volume is significantly reduced [Table 1 and ref (12)]. The density of granule cell neurons and Purkinje cells is also reduced in Ts65Dn. Cerebellar volume and granule cell density are reduced to a lesser extent in the Ts1Cje and Ms1Cje/Ts65Dn models (20).

We quantified these phenotypes in the Ts1Rhr and Ms1Rhr models. Cerebellar volume was measured by creating regions of interest in serial slices of MRIs, summing the number of voxels and normalizing to total brain volume. Despite the fact that Ts1Rhr mice are significantly larger than euploid littermates throughout life, the normalized Ts1Rhr cerebellum showed a small but significant reduction to 95% of euploid ($P = 0.003$, Table 1). This is a smaller reduction than that observed in Ts65Dn or Ts1Cje mice (88 or 89% of euploid), i.e. Ts1Rhr presents with a milder version of this phenotype.

Cell density in the internal granule and the Purkinje cell layers was determined from 10 Ts1Rhr animals and 12 euploid controls (Table 1). In contrast to Ts65Dn, granule cell density was not different from euploid in Ts1Rhr mice (102% of euploid, $P = 0.41$). Purkinje cell density was also the same as euploid in Ts1Rhr mice (101%, $P = 0.86$).

Segmental monosomy produces a novel cerebellar phenotype

Monosomy is generally more detrimental to viability and development of animals than is trisomy (30). Ms1Rhr mice are viable but cannot be inbred and are significantly smaller than euploid from birth. Cerebellar volume was measured in 10 Ms1Rhr animals and 11 euploid controls and normalized to brain volume (Table 1). In contrast to trisomic mouse strains Ts65Dn, Ts1Cje and Ts1Rhr, which each have a small cerebellum relative to euploid, the Ms1Rhr cerebellum is significantly larger than that of euploid littermates (104%, $P = 0.008$) and has a higher density of both granule and Purkinje cells (Table 1), thus the number of these neurons is further increased. Granule cell density was 115% of euploid ($P = 0.002$) and Purkinje cell density was 116% of the euploid values in the Ms1Rhr cerebellum ($P = 0.002$).

'DSCR' is not sufficient to impair hippocampal function

Cognitive impairment in individuals with DS is especially pronounced in tasks requiring hippocampal function (15–17). Ts65Dn mice also have a robust impairment of hippocampal function as measured in tests such as the Morris water maze (15–17). The DSCR hypothesis predicts that trisomy for genes in this segment is sufficient to produce mental retardation of the DS type and thus, Ts1Rhr mice should show the same effects in the Morris maze as Ts65Dn. Unlike the other aneuploid models studied here, Ts1Rhr can be inbred. This allowed us to eliminate genetic background differences as a source of variation in swim test

Table 1. Relative measures of brain phenotypes in aneuploid mice, percent of euploid[a,b]

	Ts1Rhr	Ms1Rhr	Ts65Dn
Normalized cerebellar volume index[c]	95% (0.94) $n = 10$ Ts1Rhr $n = 11$ euploid $P = 0.003$	104% (0.71) $n = 10$ Ms1Rhr $n = 11$ euploid $P = 0.008$	88% (2.1) $n = 10$ Ts65Dn $n = 10$ euploid $P = 0.0003$
Normalized hippocampal volume index	102% (2.79) $n = 10$ Ts1Rhr $n = 11$ euploid $P = 0.58$	51% (2.2) $n = 10$ Ms1Rhr $n = 11$ euploid $P < 0.001$	100% (2.47) $n = 7$ Ts65Dn $n = 6$ euploid $P = 0.95$
Cerebellar granule cell density index[c]	102% (1.53) $n = 10$ Ts1Rhr $n = 12$ euploid $P = 0.41$	115% (3.84) $n = 8$ Ms1Rhr $n = 12$ euploid $P = 0.002$	76% (4.74) $n = 8$ Ts65Dn $n = 8$ euploid $P = 0.0001$
Cerebellar Purkinje cell density index[c]	101% (1.44) $n = 10$ Ts1Rhr $n = 12$ euploid $P = 0.86$	116% (2.83) $n = 8$ Ms1Rhr $n = 12$ euploid $P = 0.002$	90% (3.88) $n = 6$ Ts65Dn $n = 6$ euploid $P = 0.03$

[a]Two tailed *t*-test between aneuploid and euploid animals for the specific strain.
[b]Standard error of the mean is indicated in parentheses.
[c]Values for Ts65Dn from Baxter *et al*. (12).

results. No difference was seen between B6.Ts1Rhr mice and euploid littermates in the visible or hidden platform test of the Morris maze (Fig. 3A and B). All behavioral testing was done with male mice only.

In Ts65Dn and Ts1Cje mice, Morris maze deficits correlate with deficits in evoked LTP but normal neurotransmission in hippocampus (23,26,31). To further characterize the hippocampal learning and memory phenotype of the Ts1Rhr mouse, we measured LTP in the CA1 area. As expected, orthodromically evoked field excitatory postsynaptic potentials (fEPSPs) (baseline) recorded from the CA1 area revealed no difference between male euploid ($n = 9$) and Ts1Rhr ($n = 12$) mice ($P > 0.25$; Fig. 3C).

After at least 30 min of stable baseline, the LTP paradigm was applied and fEPSPs were recorded for a further 60 min. Throughout the 60 min following the high-frequency tetanus, responses from 12 slices from Ts1Rhr hippocampi showed no significant difference in potentiation when compared with the nine slices from euploid hippocampi ($P = 0.69$) (Fig. 3D). In other words, no LTP impairment was detected in the Ts1Rhr CA1 area, consistent with normal spatial learning that we found in these mice. Thus, trisomy for a gene or genes in this region is not sufficient to produce deficits in this hippocampal-based task and this prediction of the DSCR hypothesis was not supported.

Hippocampal function in Ms1Rhr and Ms1Rhr/Ts65Dn mice

Neither Ms1Rhr nor Ts65Dn mice can be inbred, so both are maintained as an advanced intercross on the (B6xC3H) genetic background. Accordingly, we used a separate genetic cross to ask whether genes in the Ts1Rhr region are necessary to produce a deficit in the Morris maze. Ms1Rhr mice were crossed to Ts65Dn to produce aneusomic male mice with one, two or three copies of the DSCR for testing (Fig. 1).

Ts65Dn mice were markedly impaired in this test as expected. However, when the ca 33 conserved genes in the DSCR were returned to normal dosage in Ms1Rhr/Ts65Dn mice, these trisomic animals performed the same as euploid in the visible and hidden platform test (Fig. 4). In combination, behavior results for Ts1Rhr and Ms1Rhr/Ts65Dn mice show that a DSCR gene or genes are necessary but not sufficient to create the hippocampal dysfunction that is seen in Ts65Dn mice. Despite the significantly reduced size of the hippocampus in Ms1Rhr, the small number of monosomic mice recovered in this cross performed as well as euploid in this task (Fig. 4), suggesting that reduced dosage of these genes is not detrimental to function of the hippocampus.

DISCUSSION

Mouse models play a crucial role in understanding the gene–phenotype relationship in DS as they undergo genetically regulated developmental processes that are fundamentally similar to those in human beings. Consequently, they are frequently affected in a similar way by corresponding trisomies. We reported previously that Ts1Cje mice, which are trisomic for 78% of the genes triplicated in Ts65Dn, show somewhat milder versions of structural features of trisomy, including reduced cerebellar volume, granule cell and Purkinje cell populations, as well as features of the craniofacial skeleton. Ts1Rhr mice are trisomic for a still smaller subset of the genes triplicated Ts65Dn and Ts1Cje. They show a very mild version of the reduced cerebellar volume seen in these more complex trisomies but no effect on neuronal populations (Table 1), raising the question of whether the small trisomy elicits the same pathogenic processes. In this regard, Ts1Rhr produces a craniofacial phenotype that is clearly distinct from the larger trisomies with overall overgrowth rather than undergrowth affecting a different subset of bones in the craniofacial skeleton (20).

We found no correlation between hippocampal function (measured in the Morris water maze or by electrophysiology), the degree of effect on structural phenotype (volume and cellularity of whole brain, hippocampus and cerebellum) and the number of genes at dosage imbalance. For the small aneusomies, Ts1Rhr and Ms1Rhr, the functional impairment characteristic of Ts65Dn was not seen whether the genes were present in one or three copies. It is notable that the small segmental monosomy in Ms1Rhr mice produced some of the most striking structural changes in hippocampus of any of the aneuploid models, but these mice performed like euploid in the Morris maze.

Individuals with DS—and Ts65Dn mice—are especially affected in tasks involving the hippocampus (6). We used the Morris water maze as a test for hippocampal function in mice. Performance in this test can also be affected by cerebellar defects, unrelated to swimming coordination or speed (32). This has been associated with a reduced number of Purkinje cells; however, a robust effect in the hidden platform task was only seen when Purkinje cell loss was nearly 100%

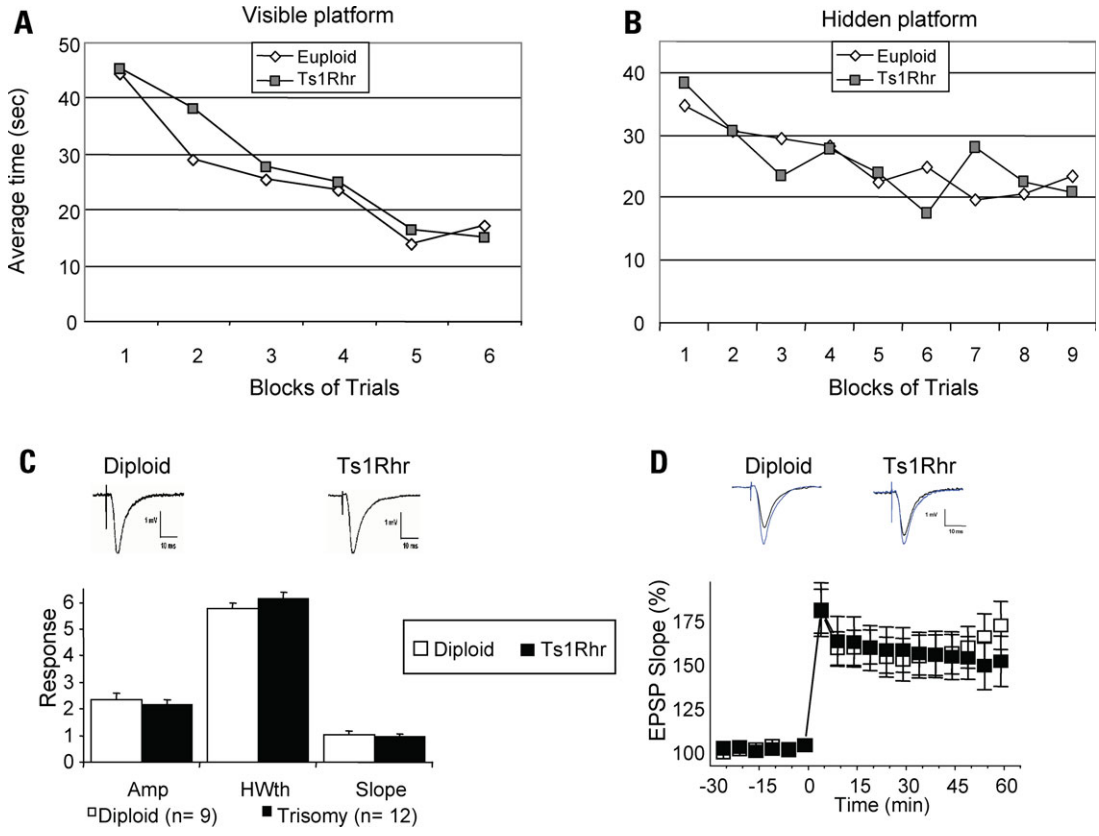

Figure 3. Trisomy for Ts1Rhr genes is not sufficient to produce the deficit in hippocampal function predicted by the DSCR hypothesis. Morris maze results for (**A**) visible and (**B**) hidden platforms, B6.Ts1Rhr ($n = 11$) versus euploid ($n = 11$) littermates (ANOVA: $P = 0.36$ and 0.72, respectively). (**C**) Representative traces of extracellular excitatory postsynaptic potentials measured from the CA1 region of the hippocampus in diploid and Ts1Rhr mice. Average amplitude, half-width and slope were normal in Ts1Rhr mice. Mean values ± SEMs are plotted. (**D**) LTP was normal in Ts1Rhr. Mean ± SEM is plotted. Representative waveforms after tetanus (1 s; 100 Hz) from diploid and Ts1Rhr are overlaid. Bars represent 1 mV and 10 ms. Open squares represent data from nine diploid mice and filled squares represent data from 12 Ts1Rhr mice.

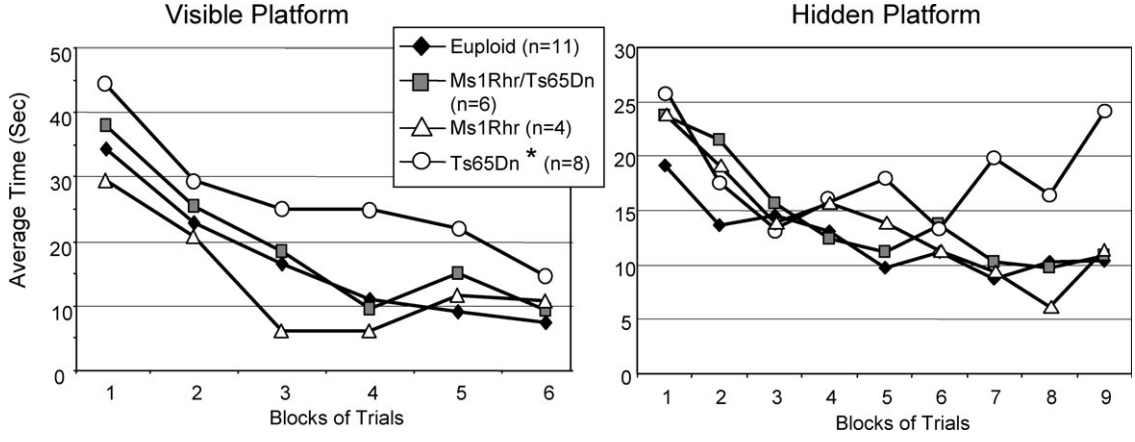

Figure 4. Trisomy for a gene or genes in the DSCR is necessary to produce a hippocampal deficit in Ts65Dn mice. Morris maze results for the visible and hidden platform tests show significant (*) impairment of Ts65Dn ($n = 8$) when compared with euploid ($n = 11$), but no difference between euploid and either Ms1Rhr/Ts65Dn ($n = 6$) or Ms1Rhr ($n = 4$). Using ANOVA and multiple comparisons testing, $\alpha = 0.05$, Ts65Dn > euploid = Ms1Rhr/Ts65Dn = Ms1Rhr for both visible and hidden platform tests.

(33). Ts65Dn mice have a ~10% reduction in Purkinje cells, whereas Ts1Rhr shows no difference from euploid and Ms1Rhr mice have higher than euploid Purkinje cell density (Table 1).

Triplication in Ts1Rhr mice of the genes corresponding to the DSCR on Hsa21 had no effect on performance in the Morris maze or on hippocampal LTP. In other words, trisomy for the DSCR was not sufficient to impair hippocampal

function and thus this prediction of the DSCR hypothesis is refuted in the mouse. This result is in contrast to reports in which mice transgenic for individual genes from this region, such as *SIM2* and *DYRK1A*, have shown variable deficits in spatial memory in the Morris water maze (34–36). Ts1Rhr mice are trisomic for these and additional genes. Returning dosage of the ca 33 DSCR genes to normal in trisomic Ms1Rhr/Ts65Dn mice (and consequently reducing the total number of conserved trisomic genes from 104 to 70) reversed the Morris maze impairment of Ts65Dn. Thus, trisomy for this segment is necessary to produce hippocampal impairment. Neither the Ts1Rhr nor Ms1Rhr/Ts65Dn mice reproduced the Ts65Dn deficit, indicating the need for complementary gene actions to produce this higher order phenotype.

The origin of the cerebellar hypoplasia in Ts65Dn mice has been traced to attenuated cell division of granule cell precursors (gcps) in early postnatal cerebellum (37). Genetic experiments and *in vitro* culture of purified gcp demonstrated that reduced mitosis is due to a cell-autonomous deficit in response to the Sonic hedgehog (SHH) growth factor. Treatment of trisomic mice with an agonist of the hedgehog pathway on the day of birth eliminated both the mitotic and gcp deficits measured 1 week later. Although this phenotype-based study produced a useful description of pathogenesis supporting a potential approach to therapies, the genetic mechanism that underlies the cell-autonomous SHH response deficit of gcp is unknown. In this regard, it is notable that monosomy in the Ms1Rhr mouse resulted in the opposite effects from trisomy, that is, increased cerebellar volume and increased density of both granule and Purkinje cells. This raises the possibility that this region contains a gene or genes that are dosage sensitive in both directions, making cells more sensitive to the mitogenic effects of SHH when under-expressed and less sensitive when over-expressed (at least in the context of a larger trisomy). As noted in the prior study, a case could be made for a contribution of attenuated SHH response in several phenotypes of DS (37).

Ever since the discovery by Lejeune *et al.* (38) that trisomy 21 is the cause of DS, efforts have been made to attribute the increased expression of individual genes to specific clinical phenotypes of the syndrome. This is clear if simplistic approach drove much of the gene discovery effort that was a major focus of DS research until the finished sequence for Hsa21 and the attendant gene catalog became available in 2000 (39). Phenotype maps defining 'critical regions' played an important role in this effort. Indeed, some studies in mice demonstrate significant contributions to specific phenotypes by single genes. For example, Mobley and co-workers used quantitative assessments of both gene expression and phenotypic outcomes to document effects of *App* gene dosage in retrograde transport of nerve growth factor. Disruption of this process is involved in the degeneration of cholinergic neurons of the basal forebrain (40). These authors are careful to point out that *App* dosage alone is not sufficient to produce the same degree of effect as seen in trisomic mice, i.e. dosage effects of this single gene produce a significant but partial phenotype in their models. Thus, even in this precisely defined case, the uni-dimensional nature of a 'one gene–one phenotype' approach exemplified by the critical region hypothesis does not adequately describe the phenotypic outcome of the experiment. Rather, the phenotypic outcome is the product of dosage effects of multiple genes affecting developmental processes and functions, a condition that argues strongly against a simple one gene–one phenotype explanation for the myriad effects seen in DS (20,28,41,42).

This report combined with previous studies (28) effectively disproves the contention of the DSCR hypothesis that one or a few genes are sufficient to account for pathogenesis resulting in the production of a number of major, complex DS phenotypes. Accordingly, the misleading DSCR nomenclature should be avoided. The observation that one or more of the 33 genes that are trisomic in Ts1Rhr mice are required to produce impaired cognitive function in Ts65Dn illustrates the requirement for gene interactions in forming a fully functional hippocampus and highlights the challenge of identifying sets of genes that produce phenotypes by combinatorial effects. A focus on mechanisms of pathogenesis in addition to more traditional gene-based approaches may prove to be productive for suggesting therapeutic interventions to alleviate features of DS in the near term.

MATERIALS AND METHODS

Mice

Dp(16Cbr1-ORF9)1Rhr and Del(16Cbr1-ORF9)1Rhr, referred to here as Ts1Rhr and Ms1Rhr, respectively, were produced as described (43) and maintained in our colony with food and water *ad libitum*. Both strains can be obtained from the Jackson Laboratory (Bar Harbor, ME, USA) (Stock nos 005383 and 005654, respectively) and from the European Mouse Mutant Archive. Aneuploid mice used for MRI analysis and histology were F1 animals from C57BL/6J (Jackson Laboratories) × founder chimeras, in which the modified chromosomes were present on a 129S6/SvEv genetic background (Taconic, Germantown, NY, USA). Controls were (C57BL/6J × 129S6) F1 mice providing an identical genetic background. Both males and females were used for structural studies at 8–9 weeks of age. In all other procedures, male littermate controls were used. Mice were deeply anesthetized with methoxyfluorane (Metofane, Medical Developments, Springvale, Australia) and perfused intracardially with 4% paraformaldehyde and processed for histology as described previously (12).

B6EiC3Sn *a*/*A*-T(16C3-4;17A2)65Dn/J (herein, Ts65Dn) (44) was obtained from the Jackson Laboratory and maintained as an advanced intercross with (C57BL/6J × C3H/HeJ)F_1 mice. All mice were typed for a mutant allele of retinal degeneration (rd) (44) and only those that were wild-type or rd/+ at this locus were used in behavioral testing.

Two crosses were established for the Morris water maze. B6.Ts1Rhr mice were produced by more than seven generations of backcrossing to C57BL/6J, and the performance of trisomic mice was tested relative to euploid littermates. Only male mice 8–10 weeks of age were used in this analysis. Neither Ts65Dn nor Ms1Rhr can be inbred; both are maintained as an advanced intercross (B6 × C3)F_n. Matings between male Ms1Rhr and female Ts65Dn produced Ts65Dn, Ms1Rhr, Ms1Rhr/Ts65Dn and euploid progeny as

described (20). All procedures were approved by the Institutional Animal Care and Use Committee.

Magnetic resonance imaging

Brains of Ts1Rhr and euploid controls were suspended in fomblin for imaging and vacuumed for 5–10 min to remove air bubbles. Images were obtained as described (12) using a 400 MHz Omega NMR Spectrophotometer (General Electric) interfaced to a 9.4 T/89 mm vertical bore magnet equipped with Accustar™ actively shielded gradients, with adiabatic radio frequency pulses of 2 ms duration, repetition time of 1.2 s and echo time of 80 ms. The sampling data points were $512 \times 70 \times 64$, resulting in a data matrix of $512 \times 140 \times 128$ after zero filling. The field of view was 17 mm × 11 mm × 10 mm. Images were postinterpolated to make the volumetric pixel size isotropic (33 μm^3). The investigator was blinded to the sample genotypes for both MRI collection and data analysis.

MRI images were analyzed using the MRIcro program (45) available at http://www.psychology.nottingham.ac.uk/staff/cr1/mricro.html. MRIcro allows the user to define 'regions of interest', which can be created and viewed in any dimension and then added to measure volume in each slice. Volumetric measurements were taken of cerebellum and total brain as described (20) and included both right and left halves. Regions of interest for the hippocampus were created from an adaptation of rat anatomic landmarks (29,46). The dorsal boundaries were the external capsule and corpus collosum, the lateral boundaries were the lateral ventricles and the medial and ventral boundaries were the stria medullaris and nuclei of the thalamus and stria terminalis. All subregions (oriens, CA1, CA2, CA3 and dentate gyrus) of the hippocampus as well as the fimbria were included. Volumes of the cerebellum and hippocampus were normalized by total brain volume to account for overall body size differences.

Histological analysis

Brains were embedded in paraffin and serial sections of 5 μm which spanned the midline were obtained and stained with hematoxylin and eosin. Granule cell and Purkinje cell densities were measured as described previously (20). Briefly, granule cells were counted in 12 independent, non-overlapping, randomly selected 5000 μm (2) fields from mid-sagittal cerebellar folia III, IV and V. The linear density of Purkinje cells was calculated by dividing the total number of Purkinje cells in a midline sagittal section by the length of the Purkinje layer and averaging the values for two midline sagittal sections.

Behavior analysis

Only male mice were used in these experiments. Housing conditions were maintained uniformly for all strains, including nestlets in each cage, as environmental enrichment can alter behavior of Ts65Dn mice (47). The Morris water maze (17) consists of a circular stainless steel swim tank (72 cm in diameter and 15 cm deep) filled with water made opaque by the addition of non-toxic white latex powder paint. The testing had a number of components. The first was a visible-platform task in which the position of a small platform (5 cm square), the top of which was 1 cm below the surface of the water, was signaled by the presence of a visually conspicuous 'flag' above the platform. To solve this task and swim directly to the platform, an animal needs only to learn that the flag indicates the location of the platform. The platform location varies among four possible positions within each block of trials and animals are tested on three blocks of trials per day (a total of 12 trials) for 2 days. Blocks of trials were separated by 1 h. Animals were placed into the water in the center of the tank. Latency to locate the platform and escape from the water on each trial was the dependent measure. Once the platform was located, mice were allowed to remain on the platform for 30 s before beginning the next trial. Mice were allowed to swim for a maximum of 60 s. Animals that did not find the platform within that time were placed on the platform and allowed to remain there for 30 s.

Twelve days after completion of the visible-platform task, mice were tested on the hidden platform version of the task. In this version, there was no flag identifying the position of the platform and the escape platform was maintained in a fixed location within the tank. As there were no immediate platform cues and the animal could not see the platform, the mice needed to acquire a multiple spatial between extra-maze cues and the position of the platform. Animals received three blocks of trials for 3 consecutive days on the hidden platform task. Animals were placed into the tank around the perimeter in one of four start positions that were used in a semirandom fashion throughout the four trials per block. Mice were allowed to search the tank for 60 s and allowed to remain on the platform for 30 s. If the platform was not located within 60 s, they were removed from the water and placed on the platform and allowed to remain for 30 s. Again, escape latencies were the dependent variable.

Statistical analysis for structural and behavioral studies

Volumes for each Ms1Rhr, Ts1Rhr, Ts65Dn and euploid cerebellum and hippocampus were normalized to total brain size of the animal. Ts1Rhr and Ms1Rhr normalized cerebellar size; granule and Purkinje cell densities were compared with that of euploid animals and differences were examined with a two tailed *t*-test. Granule and Purkinje cell densities were compared between Ts1Rhr or Ms1Rhr mice and their respective euploid littermates by a two tailed *t*-test. To compare aneuploid strains and control for the genetic background, an index was created by dividing the cerebellar and hippocampal volume and the number of granule and Purkinje cells from each animal by the average volume or cell number from all the euploid littermates. Analysis of variance (ANOVA) was used to assess differences between aneuploid strains. Least significant differences (*post hoc* comparisons) were performed to determine differences between strains for each phenotype (significance level $\alpha = 0.05$ was used). Data from the visible and hidden platform testing were analyzed using a factorial model ANOVA for factors of genotype and blocks of trials. Significant effects from factorial ANOVA were analyzed using least significant differences to (*post hoc* comparisons, $\alpha = 0.05$) determine differences between genotypes.

Electrophysiology

LTP was measured on hippocampal slices using standard extracellular recording and stimulating techniques (23,24). Male mice 2–3 months old were anesthetized, decapitated, the brain rapidly removed and placed in standard artificial cerebrospinal fluid (ACSF) containing (in millimolar) NaCl 124, KCl 3.25, $CaCl_2$ 2, NaH_2PO_4 1.25, $MgSO_4$ 1, $NaHCO_3$ 20, D-glucose 10 at 4°C bubbled with a mixture of 95% O_2/5% CO_2. Transverse slices, 400 μm thick, were cut on a McIlwain tissue chopper and transferred to a recording chamber at the interface between warm (30°C) ACSF (pH 7.4) and humidified gas (95% O_2/5% CO_2). The slices were superfused (2 ml/min) and allowed to equilibrate in the chamber for at least 1 h prior to recording.

Hippocampal fEPSPs, adjusted to approximately one-third of the maximal response, were recorded with a glass pipette filled with 2 M NaCl placed in the striatum radiatum and evoked from the Schaffer collateral–commissural pathway at 60 s intervals by a concentric bipolar platinum electrode. fEPSPs were digitized online using LTP-acquisition software (9). LTP (NMDA receptor-dependent, block by AP5, a NMDA receptor-specific antagonist) was induced by a 100-pulse train at 100 Hz from the stimulating electrode. One slice was used per animal, and experiments were performed without prior knowledge of the genotype. In all experiments, fEPSPs were quantified by averaging five consecutive waveforms and measuring the initial slope.

Differences between mean fEPSP changes after tetanizing pulses to diploid and Ts1Rhr mice were assessed using repetitive measure ANOVA, and differences in the waveforms were assessed using the Mann–Whitney rank sum test. Values are given as mean ± SEM, and statistical significance was taken as $P < 0.05$.

ACKNOWLEDGEMENTS

We thank V.P. Chacko, S. Mori and R. Xue for MRI collection and N. Rao for assisting in MRI analysis. L.E.O. was supported by a Howard Hughes Predoctoral Fellowship. This work was supported by National Research Service Award HD43614 (to R.J.R.); the J. LeJeune Foundation and USUHS (to Z.G.) and Public Health Service Awards HD38417 (to Z.G.) and HD38384 (to R.H.R.).

Conflict of Interest statement. The authors declare that they have no conflicts of interest.

REFERENCES

1. Kahlem, P., Sultan, M., Herwig, R., Steinfath, M., Balzereit, D., Eppens, B., Saran, N.G., Pletcher, M.T., South, S.T., Stetten, G. *et al*. (2004) Transcript level alterations reflect gene dosage effects across multiple tissues in a mouse model of down syndrome. *Genome Res.*, **14**, 1258–1267.
2. Lyle, R., Gehrig, C., Neergaard-Henrichsen, C., Deutsch, S. and Antonarakis, S.E. (2004) Gene expression from the aneuploid chromosome in a trisomy mouse model of down syndrome. *Genome Res.*, **14**, 1268–1274.
3. Nikolaienko, O., Nguyen, C., Crinc, L.S., Cios, K.J. and Gardiner, K. (2005) Human chromosome 21/Down syndrome gene function and pathway database. *Gene*, **364**, 90–98.
4. Delabar, J.M., Theophile, D., Rahmani, Z., Chettouh, Z., Blouin, J.L., Prieur, M., Noel, B. and Sinet, P.M. (1993) Molecular mapping of twenty-four features of Down syndrome on chromosome 21. *Eur. J. Hum. Genet.*, **1**, 114–124.
5. Korenberg, J. (1991) Down syndrome phenotype mapping. In Epstein, C. (ed.), *Progress in Clinical and Biological Research*. Wiley-Liss, New York, Vol. **373**, pp. 43–52.
6. Pennington, B.F., Moon, J., Edgin, J., Stedron, J. and Nadel, L. (2003) The neuropsychology of Down syndrome: evidence for hippocampal dysfunction. *Child Dev.*, **74**, 75–93.
7. White, N.S., Alkire, M.T. and Haier, R.J. (2003) A voxel-based morphometric study of nondemented adults with Down Syndrome. *Neuroimage*, **20**, 393–403.
8. Teipel, S.J., Schapiro, M.B., Alexander, G.E., Krasuski, J.S., Horwitz, B., Hoehne, C., Moller, H.J., Rapoport, S.I. and Hampel, H. (2003) Relation of corpus callosum and hippocampal size to age in nondemented adults with Down's syndrome. *Am. J. Psychiatry*, **160**, 1870–1878.
9. Aylward, E.H., Li, Q., Honeycutt, N.A., Warren, A.C., Pulsifer, M.B., Barta, P.E., Chan, M.D., Smith, P.D., Jerram, M. and Pearlson, G.D. (1999) MRI volumes of the hippocampus and amygdala in adults with Down's syndrome with and without dementia. *Am. J. Psychiatry*, **156**, 564–568.
10. Pinter, J.D., Brown, W.E., Eliez, S., Schmitt, J.E., Capone, G.T. and Reiss, A.L. (2001) Amygdala and hippocampal volumes in children with Down syndrome: a high-resolution MRI study. *Neurology*, **56**, 972–974.
11. Jernigan, T.L. and Bellugi, U. (1990) Anomalous brain morphology on magnetic resonance images in Williams syndrome and Down syndrome. *Arch. Neurol.*, **47**, 529–533.
12. Baxter, L.L., Moran, T.H., Richtsmeier, J.T., Troncoso, J. and Reeves, R.H. (2000) Discovery and genetic localization of Down syndrome cerebellar phenotypes using the Ts65Dn mouse. *Hum. Mol. Genet.*, **9**, 195–202.
13. Roper, R., St John, H., Philip, J., Lawler, A. and Reeves, R. (2006) Perinatal loss of Ts65Dn mice, a model of Down syndrome. *Genetics*, **172**, 437–443.
14. Richtsmeier, J., Baxter, L. and Reeves, R. (2000) Parallels of craniofacial maldevelopment in Down Syndrome and Ts65Dn mice. *Dev. Dyn.*, **217**, 137–145.
15. Escorihuela, R.M., Fernandez-Teruel, A., Vallina, I.F., Baamonde, C., Lumbreras, M.A., Dierssen, M., Tobena, A. and Florez, J. (1995) A behavioral assessment of Ts65Dn mice: a putative Down syndrome model. *Neurosci. Lett.*, **199**, 143–146.
16. Holtzman, D.M., Santucci, D., Kilbridge, J., Chua-Couzens, J., Fontana, D.J., Daniels, S.E., Johnson, R.M., Chen, K., Sun, Y., Carlson, E. *et al*. (1996) Developmental abnormalities and age-related neurodegeneration in a mouse model of Down syndrome. *Proc. Natl Acad. Sci. USA*, **93**, 13333–13338.
17. Reeves, R., Irving, N., Moran, T., Wohn, A., Kitt, C., Sisodia, S., Schmidt, C., Bronson, R. and Davisson, M. (1995) A mouse model for Down syndrome exhibits learning and behaviour deficits. *Nat. Genet.*, **11**, 177–183.
18. Sago, H., Carlson, E.J., Smith, D.J., Kilbridge, J., Rubin, E.M., Mobley, W.C., Epstein, C.J. and Huang, T.T. (1998) Ts1Cje, a partial trisomy 16 mouse model for Down syndrome, exhibits learning and behavioral abnormalities. *Proc. Natl Acad. Sci. USA*, **95**, 6256–6261.
19. Richtsmeier, J.T., Zumwalt, A., Carlson, E.J., Epstein, C.J. and Reeves, R.H. (2002) Craniofacial phenotypes in segmentally trisomic mouse models for Down syndrome. *Am. J. Med. Genet.*, **107**, 317–324.
20. Olson, L.E., Roper, R.J., Baxter, L.L., Carlson, E.J., Epstein, C.J. and Reeves, R.H. (2004) Down syndrome mouse models Ts65Dn, Ts1Cje, and Ms1Cje/Ts65Dn exhibit variable severity of cerebellar phenotypes. *Dev. Dyn.*, **230**, 581–589.
21. Insausti, A.M., Megias, M., Crespo, D., Cruz-Orive, L.M., Dierssen, M., Vallina, I.F., Insausti, R., Florez, J. and Vallina, T.F. (1998) Hippocampal volume and neuronal number in Ts65Dn mice: a murine model of Down syndrome. *Neurosci. Lett.*, **253**, 175–178.
22. Lorenzi, H.A. and Reeves, R.H. (2006) Hippocampal hypocellularity in the Ts65Dn mouse originates early in development. *Brain Res.*, **1104**, 153–159.
23. Siarey, R.J., Carlson, E.J., Epstein, C.J., Balbo, A., Rapoport, S.I. and Galdzicki, Z. (1999) Increased synaptic depression in the Ts65Dn mouse, a model for mental retardation in Down syndrome. *Neuropharmacology*, **38**, 1917–1920.

24. Siarey, R.J., Villar, A.J., Epstein, C.J. and Galdzicki, Z. (2005) Abnormal synaptic plasticity in the Ts1Cje segmental trisomy 16 mouse model of Down syndrome. *Neuropharmacology*, **49**, 122–128.
25. Costa, A.C. and Grybko, M.J. (2005) Deficits in hippocampal CA1 LTP induced by TBS but not HFS in the Ts65Dn mouse: a model of Down syndrome. *Neurosci. Lett.*, **382**, 317–322.
26. Kleschevnikov, A.M., Belichenko, P.V., Villar, A.J., Epstein, C.J., Malenka, R.C. and Mobley, W.C. (2004) Hippocampal long-term potentiation suppressed by increased inhibition in the Ts65Dn mouse, a genetic model of Down syndrome. *J. Neurosci.*, **24**, 8153–8160.
27. O'Doherty, A., Ruf, S., Mulligan, C., Hildreth, V., Errington, M.L., Cooke, S., Sesay, A., Modino, S., Vanes, L., Hernandez, D. *et al*. (2005) An aneuploid mouse strain carrying human chromosome 21 with down syndrome phenotypes. *Science*, **309**, 2033–2037.
28. Olson, L.E., Richtsmeier, J.T., Leszl, J. and Reeves, R.H. (2004) A chromosome 21 critical region does not cause specific down syndrome phenotypes. *Science*, **306**, 687–690.
29. Wolf, O.T., Dyakin, V., Vadasz, C., de Leon, M.J., McEwen, B.S. and Bulloch, K. (2002) Volumetric measurement of the hippocampus, the anterior cingulate cortex, and the retrosplenial granular cortex of the rat using structural MRI. *Brain Res. Brain Res. Protoc.*, **10**, 41–46.
30. Sandler, L. and Hecht, F. (1973) Annotation: genetic effects of aneuploidy. *Am. J. Hum. Genet.*, **25**, 332–339.
31. Siarey, R.J., Stoll, J., Rapoport, S.I. and Galdzicki, Z. (1997) Altered long-term potentiation in the young and old Ts65Dn mouse, a model for Down Syndrome. *Neuropharmacology*, **36**, 1549–1554.
32. Lalonde, R. and Strazielle, C. (2003) The effects of cerebellar damage on maze learning in animals. *Cerebellum*, **2**, 300–309.
33. Martin, L.A., Goldowitz, D. and Mittleman, G. (2003) The cerebellum and spatial ability: dissection of motor and cognitive components with a mouse model system. *Eur. J. Neurosci.*, **18**, 2002–2010.
34. Altafaj, X., Dierssen, M., Baamonde, C., Marti, E., Visa, J., Guimera, J., Oset, M., Gonzalez, J.R., Florez, J., Fillat, C. *et al*. (2001) Neurodevelopmental delay, motor abnormalities and cognitive deficits in transgenic mice overexpressing Dyrk1A (minibrain), a murine model of Down's syndrome. *Hum. Mol. Genet.*, **10**, 1915–1923.
35. Ema, M., Ikegami, S., Hosoya, T., Mimura, J., Ohtani, H., Nakao, K., Inokuchi, K., Katsuki, M. and Fujii-Kuriyama, Y. (1999) Mild impairment of learning and memory in mice overexpressing the mSim2 gene located on chromosome 16: an animal model of Down's syndrome. *Hum. Mol. Genet.*, **8**, 1409–1415.
36. Smith, D.J., Stevens, M.E., Sudanagunta, S.P., Bronson, R.T., Makhinson, M., Watabe, A.M., O'Dell, T.J., Fung, J., Weier, H.U., Cheng, J.F. *et al*. (1997) Functional screening of 2 Mb of human chromosome 21q22.2 in transgenic mice implicates minibrain in learning defects associated with Down syndrome. *Nat. Genet.*, **16**, 28–36.
37. Roper, R.J., Baxter, L.L., Saran, N.G., Klinedinst, D.K., Beachy, P.A. and Reeves, R.H. (2006) Defective cerebellar response to mitogenic Hedgehog signaling in Down syndrome mice. *Proc. Natl Acad. Sci. USA*, **103**, 1452–1456.
38. Lejeune, J., Gauthier, M. and Turpin, R. (1959) Etudes des chromosomes somatiques de neuf enfants mongoliens. *CR Acad. Sci. (Paris)*, **248**, 1721–1722.
39. Hattori, M., Fujiyama, A., Taylor, T.D., Watanabe, H., Yada, T., Park, H.S., Toyoda, A., Ishii, K., Totoki, Y., Choi, D.K. *et al*. (2000) The DNA sequence of human chromosome 21. *Nature*, **405**, 311–319.
40. Salehi, A., Delcroix, J.D., Belichenko, P.V., Zhan, K., Wu, C., Valletta, J.S., Takimoto-Kimura, R., Kleschevnikov, A.M., Sambamurti, K., Chung, P.P. *et al*. (2006) Increased App expression in a mouse model of Down's syndrome disrupts NGF transport and causes cholinergic neuron degeneration. *Neuron*, **51**, 29–42.
41. Potier, M.C., Rivals, I., Mercier, G., Ettwiller, L., Moldrich, R.X., Laffaire, J., Personnaz, L., Rossier, J. and Dauphinot, L. (2006) Transcriptional disruptions in Down syndrome: a case study in the Ts1Cje mouse cerebellum during post-natal development. *J. Neurochem.*, **97** (Suppl. 1), 104–109.
42. Roper, R. and Reeves, R. (2006) Understanding the basis for Down syndrome phenotypes. *PLoS Genet.*, **2**, 231–236.
43. Olson, L.E., Richtsmeier, J.T., Leszl, J. and Reeves, R.H. (2004) A chromosome 21 critical region does not cause specific down syndrome phenotypes. *Science*, **306**, 687–690.
44. Baehr, W., Champagne, M.S., Lee, A.K. and Pittler, S.J. (1991) Complete cDNA sequences of mouse rod photoreceptor cGMP phosphodiesterase alpha- and beta-subunits, and identification of beta′-, a putative beta-subunit isozyme produced by alternative splicing of the beta-subunit gene. *FEBS Lett.*, **278**, 107–114.
45. Rorden, C. and Brett, M. (2000) Stereotaxic display of brain lesions. *Behav. Neurol.*, **12**, 191–200.
46. Paxinos, G. and Franklin, K.B.J. (2001) *The Mouse Brain in Stereotaxic Coordinates*, 2nd edn. Academic Press, San Diego.
47. Martinez-Cue, C., Baamonde, C., Lumbreras, M., Paz, J., Davisson, M.T., Schmidt, C., Dierssen, M. and Florez, J. (2002) Differential effects of environmental enrichment on behavior and learning of male and female Ts65Dn mice, a model for Down syndrome. *Behav. Brain Res.*, **134**, 185–200.